# JIGSAWCOMM: Joint Semantic Feature Encoding and Transmission for Communication-Efficient Cooperative Perception

Chenyi Wang<sup>1</sup> Zhaowei Li<sup>2</sup> Ming F. Li<sup>1</sup> Wujie Wen<sup>2</sup>
<sup>1</sup>University of Arizona <sup>2</sup>North Carolina State University

{chenyiw, lim}@arizona.edu {zli223, wwen2}@ncsu.edu

#### **Abstract**

Multi-agent cooperative perception (CP) promises to overcome the inherent occlusion and sensing-range limitations of single-agent systems (e.g. autonomous driving). However, its practicality is severely constrained by the limited communication bandwidth. Existing approaches attempt to improve bandwidth efficiency via compression or heuristic message selection, without considering the semantic relevance or cross-agent redundancy of sensory data. We argue that a practical CP system must maximize the contribution of every transmitted bit to the final perception task, by extracting and transmitting semantically essential and non-redundant data. In this paper, we formulate a joint semantic feature encoding and transmission problem, which aims to maximize CP accuracy under limited bandwidth. To solve this problem, we introduce JigsawComm, an end-to-end trained, semantic-aware, and communication-efficient CP framework that learns to "assemble the puzzle" of multiagent feature transmission. It uses a regularized encoder to extract semantically-relevant and sparse features, and a lightweight Feature Utility Estimator to predict the contribution of each agent's features to the final perception task. The resulting meta utility maps are exchanged among agents and leveraged to compute a provably optimal transmission policy, which selects features from agents with the highest utility score for each location. This policy inherently eliminates redundancy and achieves a scalable O(1) communication cost as the number of agents increases. On the benchmarks OPV2V and DAIR-V2X, JigsawComm reduces the total data volume by up to >500× while achieving matching or superior accuracy compared to state-of-the-art methods.

### 1. Introduction

Multi-agent cooperative perception (CP) enables connected road agents, such as connected and autonomous vehicles (CAVs) and road-side units (RSUs), to improve their understanding of the environment [14]. By leveraging sensor

data exchanged through Vehicle-to-Everything (V2X) communication [5], participating agents can detect objects beyond their individual sensing ranges, minimize blind spots, and perceive occluded obstacles [33]. With its great potential for facilitating more informed driving decisions and enhancing road safety, CP is a critical technology for 50–90% of the vehicle market that CAVs are anticipated to comprise by 2040 [2].

Despite this promise, CP faces a formidable challenge in communication efficiency. The available V2X bandwidth is severely limited (up to 20 MHz for both DSRC [7] and C-V2X [6]), while the volume of sensor data generated is prohibitively large (e.g. 4 MB per LiDAR frame [3]). Exchanging raw sensor data is therefore infeasible while satisfying the stringent real-time perception requirements of autonomous driving (e.g. <100 ms [16]). As previous research also demonstrated that exchanging local detection results alone is suboptimal [33], the field has largely converged on the intermediate fusion framework—exchanging and fusing Bird's-Eye-View (BEV) features—as the most effective paradigm [33]. Even so, transmitting dense deep features from multiple agents still exhausts V2X bandwidth.

The key challenge stems from the high degree of data redundancy present in these shared features, which can be classified into two forms: (i) Intra-agent redundancy, where features waste bits on semantically irrelevant information; and (ii) Inter-agent redundancy, where multiple agents transmit overlapping and unnecessary information. As shown in Fig. 1, under limited bandwidth, such inefficient communication not only leads to reduced detection coverage but can even degrade perception accuracy when lower quality data dilutes the utility of the better ones after fusion.

Existing work on communication-efficient CP fails to solve this. They typically adopt one of two strategies: (i) Compression methods, such as encoder-decoders [33] or codebooks [10, 39]. Such methods either only reduce the data size but still transmit the entire feature map, failing to address redundancy, or overly restrict the representation power to offline-trained dictionaries, undermining generalizability; (ii) Message selection methods [9, 10, 18, 30],



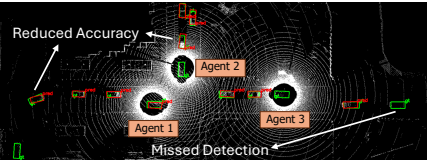




Figure 1. A sample scenario from OPV2V dataset (left). Under the same bandwidth limit, prior work [9] (mid) does not utilize bandwidth efficiently, leading to missed detection and reduced accuracy. JIGSAWCOMM (right) maximizes every bit's contribution, enabling complete and accurate detection. Quantitative evaluation and discussion on the 'cost' of redundancy can be found in Sec. 4 and Sec. 5, respectively.

choosing 'critical' regions to transmit but relying on simple local heuristics (e.g. local detection confidence) that are poor proxies for the final cooperative task. Crucially, both approaches ignore cross-agent redundancy. As a result, they still require significant bandwidth and are not scalable: their communication cost grows linearly with the number of agents. The problem of designing a truly communication-efficient, scalable, and accurate CP system remains open.

To design such a CP system, we argue that it must maximize the contribution of every transmitted bit towards the final perception goal. This requires that only essential, semantically meaningful, and non-redundant information is transmitted. Therefore, the feature encoding (local compression) and transmission (message selection) algorithms must be jointly designed to realize this potential. This joint design is non-trivial. Removing semantic, cross-agent redundancy is a challenging 'chicken-and-egg' problem: an agent cannot determine if its features are redundant without first knowing what other agents intend to transmit.

To address these gaps, we propose JigsawComm, an endto-end semantic-aware CP framework that learns to "assemble the puzzle" of multi-agent feature transmission. Our approach is based on the joint semantic feature encoding and transmission problem that we formulate. First, a regularized feature encoder is trained to extract features that are both semantically important and sparse. Second, a lightweight Feature Utility Estimator (FUE) head is introduced to predict the data utility of each agent's feature to the final perception result, producing compact meta utility maps that (i) approximate the marginal contribution of each agent's features in the BEV grid to the downstream task and (ii) expose cross-agent feature overlap. This entire framework is trained end-to-end, using a differentiable scheduler to jointly optimize the feature encoder and the FUE. During inference, agents exchange the meta utility maps and locally compute an explainable, deterministic transmission policy: select at most one agent with the highest utility per cell, and greedily admit cells until the communication budget is met, which is provably optimal under our optimization formulation.

JIGSAWCOMM's transmission policy inherently eliminates cross-agent duplication by construction with its top-1 percell rule. This makes the system practical and scalable: because the final transmission is a sparse 'jigsaw' assembled from the best cell-level features across the network, the total

communication cost is bounded by the size of a single sparse feature map. This achieves an asymptotic transmission cost of  $\mathcal{O}(1)$  with respect to the number of agents N, rather than the  $\mathcal{O}(N)$  of naive broadcast. The scheduler requires only the exchanged meta utility maps and yields identical decisions across all agents, making it deployable even in the challenging decentralized mode of V2X.

Our contributions can be summarized as follows:

- We propose JigsawComm, a novel communication-efficient CP framework that maximizes the contribution of each transmitted bit to the final perception task, using a jointly trained semantic sparse feature encoder and end-to-end differentiable scheduler.
- We introduce a learned utility proxy and a deterministic, provably optimal top-1 scheduling policy that, effectively eliminates cross-agent redundancy, achieving scalable  $\mathcal{O}(1)$  communication cost.
- We extensively evaluate JigsawComm on the OPV2V and DAIR-V2X benchmarks, demonstrating comparable or superior accuracy while reducing communication data volume and improving utility-per-byte both by up to over 500× compared to prior methods [3, 9, 32, 33], setting the new SOTA for communication-efficient CP.<sup>1</sup>
- Our results uncover a counterintuitive 'more is worse' effect in existing CP fusion backbones, showing that redundant multi-agent features can *degrade* accuracy rather than improve it. We highlight the need for future CP fusion architectures that can effectively leverage, instead of suffer from, redundancy.

### 2. Background and Related Work

### 2.1. Cooperative Perception Paradigms

Research in CP has explored various strategies for fusing information from multiple agents, which are primarily categorized by the stage at which fusion occurs. Early fusion involves the transmission and aggregation of raw sensor data, such as LiDAR point clouds or camera images [37, 38]. While this approach theoretically preserves the maximum amount of information, it is prohibitively expensive in terms of required communication bandwidth and is thus considered impractical for real-world V2X applications [3]. At the

<sup>&</sup>lt;sup>1</sup>Code available at https://github.com/WiSeR-Lab/JigsawComm.

other extreme, late fusion operates on the final perception outputs, where agents directly exchange local perception results [24]. This method is highly communication-efficient but suffers from significant information loss during local processing, making it difficult to resolve detection conflicts and susceptible to error propagation [33].

The dominant paradigm in modern CP is intermediate fusion, which strikes a balance between these two extremes [3, 9, 18, 30, 32, 33]. In this approach, agents first process their raw sensor data into an intermediate feature representation, typically within a shared and aligned BEV grid. These features are then exchanged and fused before being passed to a final detection head. This strategy preserves rich semantic and spatial information while being more communication-friendly than early fusion, forming the basis for most state-of-the-art methods, including JigsawComm proposed in this paper.

### 2.2. Communication-Efficient CP Strategies

Within the intermediate fusion paradigm, several previous works have focused on optimizing the trade-off between perception performance and communication cost. These efforts can be broadly classified by their core strategy.

Message Representation: Changing How Information is Encoded. This category of methods focuses on compressing the feature maps. While standard encoder-decoder models are common [30, 33], more advanced strategies have emerged. CodeFilling [10, 39], for example, uses a shared codebook (i.e. lookup table) to quantize high-dimensional features into compact integer indices. A key limitation of this approach is that the codebook is learned offline and remains static during inference. This makes them difficult to generalize to novel environments. More recently, DiffCP proposed a generative approach [19], where the sender transmits a small semantic seed, and the receiver leverages a diffusion model to reconstruct the sender's full BEV map. While achieving very low bitrates, this method incurs a substantial computational burden for the iterative denoising process, violating real-time latency constraints [16], and carries an inherent risk of "hallucination", sacrificing accuracy.

Message Selection: Deciding What to Transmit. This line of research aims to prune the information sent by agents, assuming that not all data is equally valuable. Early work like When2com [18] employed a graph neural network with a handshake mechanism to select which agents to communicate with, performing a coarse, agent-level selection. However, as V2X communication primarily relies on wireless broadcast rather than direct pairwise communications [6, 7], optimizing communication graphs does not save bandwidth in practice. A more fine-grained approach was introduced by Where2comm [9], which has become the *de facto* canonical baseline for communication-efficient CP. The idea is to generate a spatial confidence map by applying the *de*-

Table 1. Comparison with existing methods.

Method	V2X Comm. Feasibility*			General. to Unseen Scene.	Dynam. Adjust.†
DiffCP [19]	•	0	0,0		0
Codebook [10, 39]	•	•	<b>D</b> /O	0	0
When2comm [18]	0	•	$\bigcirc / \mathbb{O}$	•	0
Enc-Decoder [33]	•	•	0/0	•	0
Where2comm [9]	•	•	●/①	•	•
JIGSAWCOMM (Ours)	•	•	•	•	•

<sup>\*</sup> Refers to whether the method can meet the bandwidth constraint of V2X and is scalable.

tector head on each agent's local feature. This map serves as a heuristic to identify 'perceptually critical' regions for transmission, which achieves region-level sparsity, reducing bandwidth compared to sending dense feature maps. More recent work followed the same idea (e.g. [30] further considered intermediate-late hybrid fusion). However, these methods still rely on heuristic utility proxies, which may not be optimal for the final CP task. They also lack explicit mechanisms to suppress redundant information from multiple collaborators with overlapping observations, resulting in a non-scalable, linear increase of communication cost with respect to the number of agents.

Nevertheless, quantifying and minimizing inter-agent redundancy is a challenging problem. Prior CP schemes that consider redundancy reduction suffer from various limitations. For example, a few early fusion based CP methods adopt geometry-based heuristics (*e.g.* each agent responsible for partitioned areas that are closest to itself) [23, 29, 35, 38], which ignore sensory data content and semantics (*e.g.* occlusion), leading to potentially inaccurate results. Also, intermediate fusion-based CP methods that adopt mutual information-based metrics for redundancy reduction are computationally impractical with limited samples [28].

**Positioning Our Work.** The existing landscape of communication-efficient CP reveals a clear set of unresolved challenges: a reliance on heuristic and non-task-optimal proxies for task utility, a lack of explicit modeling and removal of semantic inter-agent redundancy, and static performance-bandwidth trade-offs imposed by fixed representation schemes. Our work addresses these gaps by introducing a semantic-aware, task-oriented, and end-to-end learned scheduling policy that is generalizable, adaptive, and efficiently manages shared communication resources among multiple agents. Table 1 provides a comparative summary.

## 3. Methodology: End-to-End Communication-Aware Cooperative Perception

#### 3.1. Problem Formulation

We consider N agents  $A = \{a_1, \dots, a_N\}$  (CAVs or RSUs, within each other's communication range) collaborating via V2X. Per cycle, agent  $a_i$  obtains raw sensor data

Refers to a method's ability to adapt to variations in available bandwidth.

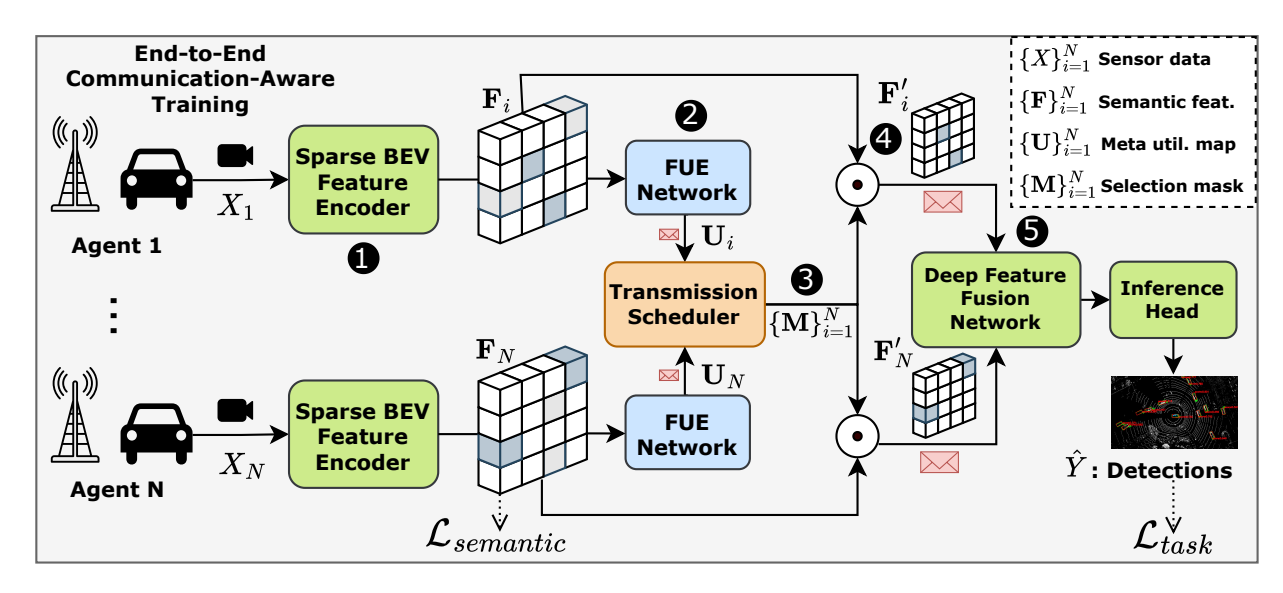


Figure 2. Overview of JigsawComm.

 $X_i$  and uses an encoder  $\Phi_{\mathrm{enc}}$  to produce a BEV feature map  $\mathbf{F}_i = \Phi_{\mathrm{enc}}(X_i) \in \mathbb{R}^{C \times H \times W}$  with cells  $\mathbf{f}_i^l \in \mathbb{R}^C$ ,  $l \in \mathcal{L} = \{1, \dots, L\}$ ,  $L{=}HW$ . After exchanging meta utility maps  $\mathbf{U}_{i=1}^N$ , each agent  $a_i$  then transmits a sparse subset  $\mathbf{F}_i' = \mathbf{M}_i \odot \mathbf{F}_i$ , where  $\mathbf{M}_i \in \{0,1\}^{H \times W}$  and  $\odot$  denotes element-wise multiplication. A fusion module  $\Phi_{\mathrm{fuse}}$  and decoder  $\Phi_{\mathrm{dec}}$  produce the output  $\hat{Y}$ . Our goal is to maximize the CP accuracy within a total communication budget  $B^2$ :

$$\max_{\theta, \{\mathbf{M}_i\}_{i=1}^N} \mathcal{P}\left(\Phi_{\text{dec}}\left(\Phi_{\text{fuse}}\left(\{\mathbf{M}_i \odot \Phi_{\text{enc}}(X_i)\}_{i=1}^N\right)\right), Y\right) \quad (1)$$
s.t. 
$$\sum_{i=1}^N |\mathbf{M}_i \odot \Phi_{\text{enc}}(X_i)| \le B. \quad (2)$$

Here,  $\mathcal{P}(\cdot)$  is the CP accuracy evaluation metric (e.g. mAP), Y corresponds to the ground truth supervision,  $\theta$  denotes the trainable parameters for the entire network, and the binary masks  $\{\mathbf{M}_i\}_{i=1}^N$  select subsets of the encoded features across spatial dimensions for transmission and fusion.

**Challenges.** This formulation presents three core challenges: (C1) During inference, since there is no ground truth, the CP accuracy  $\mathcal{P}$  cannot be directly evaluated by the agents. Thus, we must design a utility proxy that is aligned with the CP accuracy and can be computed locally. Previous work uses heuristic local confidence scores [9, 18, 25, 30], which fails to capture cross-agent redundancy and is not necessarily the optimal representations of the final accuracy. (C2) Ideally, a utility proxy needs to be jointly trained with the network under the accuracy objective to guarantee a direct alignment. However, the binary scheduling masks are *non-differentiable*, which hinders end-to-end training.

(C3) Even if the utility function can be computed or approximated, the feature selection process under Eq. (2) is combinatorial, as it reduces to a 0-1 knapsack problem, which is NP-Hard [13]. Moreover, 'more bits' is not better: redundant views congest the V2X data channel without boosting fused utility. Thus, we must transmit only *semantically meaningful*, *non-redundant* information and *maximize the contribution of every transmitted bit* to CP accuracy.

System Overview. JigsawComm learns to assemble the 'jigsaw' of multi-agent BEV features so that the CP messages carry only essential, non-overlapping content. As shown in Fig. 2, each agent: 1 produces sparse and semantically important features (Sec. 3.2); 2 predicts a compact meta utility map using a Feature Utility Estimator (FUE) network, which is exchanged among agents efficiently (Sec. 3.3); 3 locally applies a deterministic, redundancy-aware top-1-percell policy, producing a feature selection mask that maximizes the total utility while satisfying the communication budget (Sec. 3.4); 4 broadcasts the selected features; 5 fuses the exchanged features and passes to the inference head for output. With the total per-frame communication cost upper-bounded by the size of a single sparse semantic feature, the required bandwidth is  $\mathcal{O}(1)$  as the number of agents increases, ensuring high scalability.

#### 3.2. Sparse Semantic Feature Encoder

To ensure that features carry compact and *essential* semantics using a minimal number of bits, we first shape the encoder's output to reduce intra-agent redundancy. We apply a learnable threshold  $\kappa$  and a semantic loss consisting of an

 $<sup>^2{\</sup>rm In}$  practice, B equals the available bandwidth BW divided by the frame rate r (e.g. if BW=20 Mbps and r=10 FPS, B=2 Mb).

 $L_1$  regularization on the encoded feature:

$$\mathcal{L}_{\text{semantic}} = \frac{1}{NL} \sum_{i=1}^{N} \sum_{l=1}^{L} \left\| \mathbf{f}_{i}^{l} \odot \mathbb{I} \{ \mathbf{f}_{i}^{l} > \kappa \} \right\|_{1}.$$
 (3)

The  $L_1$  regularization, when applied to model parameters, is known to produce sparse coefficients, suppress irrelevant features, and shape the coefficient amplitudes based on their quantitative contribution to the final outcome [20]. However, applying  $L_1$  directly to raw activations  $\|\mathbf{f}_i^I\|_1$  only encourages small magnitudes, yet under stochastic normalization and noise, almost never yields *exact zeros*; gradients remain nonzero almost everywhere, so uninformative activations linger at small but nonzero values—still consuming bits. Therefore, we incorporate the learnable threshold  $\kappa$ , which explicitly introduces sparsity.

### 3.3. Feature Utility Estimator (FUE)

**Utility Proxy.** To address C1, we propose to maximize a utility function  $U(\cdot)$ . It represents the total contribution of all agents' transmitted data, expressed as the sum of individual agent's feature utility minus their pairwise redundancy. Essentially, our utility function can be regarded as a proxy for the overall information about the CP inference result (on the fused feature) that is contained within the transmitted data. The greater this mutual information is, the higher the perception accuracy [22, 27].

$$U^{l} = \underbrace{\sum_{i=1}^{N} m_{i}^{l} u_{i}^{l}}_{\text{importance}} - \underbrace{\sum_{j \neq i} \frac{m_{i}^{l} m_{j}^{l} \tilde{u}_{ij}^{l}}{2}}_{\text{overlap penalty}}, \tilde{u}_{ij}^{l} \triangleq \min\{u_{i}^{l}, u_{j}^{l}\}.$$

$$(4)$$

Here,  $m_i^l \in \{0,1\}$  is the binary transmission decision for  $\mathbf{f}_i^l$ ,  $u_i^l$  is its estimated importance, representing the amount of information contained in i's feature at location l about the CP inference result. Also,  $\tilde{u}_{ij}^l$  approximates the pairwise redundancy, upper-bounding the shared information that i and j's features both contain about the CP inference result, where the  $\frac{1}{2}$  factor is to avoid double-counting. Finally, the frame-level utility is  $U = \sum_{l=1}^L U^l$ .

FUE Head. To estimate the feature utility, we implement FUE as a pointwise linear decoder, similar to the architecture of a classification or regression head  $u_i^l = \operatorname{ReLU}(\mathbf{w}^{\top}\mathbf{f}_i^l + b)$ , resulting in a sparse meta utility map  $\mathbf{U}_i \in \mathbb{R}^{1 \times H \times W}$ . The layer is vectorized as a  $1 \times 1$  convolution for efficiency and interpretability, since each location already contains neighboring cells' information from the convolutional layers in the encoder. The FUE is end-to-end trained with the transmission policy described in Sec. 3.4 and aligned with the perception accuracy loss. Therefore, its value directly relates to the transmission decision such that higher utility values correlate with higher transmission priority and larger contribution to the accuracy.

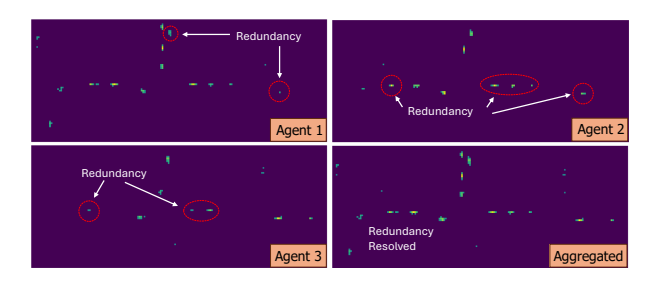


Figure 3. Visualization of meta utility map examples. The top-1 aggregated utility map eliminates redundancy by selecting the agent with the highest utility at each location.

#### 3.4. Transmission Scheduler

Even after transforming the optimization into maximizing the learned utility proxy, the challenges of non-differentiability in scheduling (C2) and the NP-hard combinatorial knapsack problem (C3) still exist. To solve these, we design a scheduling algorithm that is (i) differentiable at training and (ii) deterministic at inference with provably optimal guarantee given fixed transmission cost per feature.

After exchanging meta utility maps  $\{U_i\}_{i=1}^N$ , the scheduler produces a feature selection mask  $M_i$  for each agent based on a straightforward and interpretable policy:

- 1. For each spatial cell l, select at most one agent with the highest non-zero utility  $\max_{j} u_{i}^{l}$  to transmit.
- 2. From this set of candidates, greedily admit cells with the highest utility-to-cost ratio until the budget *B* is met.

This policy can be deterministically computed by all agents, making it practically compatible with both centralized (V2I) and decentralized (V2V) operation (Sec. 5).

**Train-Time Differentiable Scheduling.** To address C2, we relax the discrete selection during training. Instead, we model the mask  $m_i^l$  as the composition of two gates:

- (1) Importance gate (scalar, per agent–cell). We use a logistic gate with temperature  $\eta>0$ :  $\alpha_i^l=\sigma\Big(\frac{u_i^l-\tau}{\eta}\Big)$ , where  $\sigma(\cdot)$  is the sigmoid function and  $\tau$  is a learnable threshold. We anneal  $\eta\downarrow 0$  over training to make  $\alpha_i^l$  near-binary.
- (2) Cross-agent top-1 (categorical, per cell). To model the "pick one agent per cell" constraint differentiably, we apply the Gumbel–Softmax reparameterization [11] on the vector of scores  $\mathbf{u}^l=(u^l_1,\dots,u^l_N)$  with an independent Gumbel noise per agent:  $g^l_i\sim \mathrm{Gumbel}(0,1)$  with  $g^l_i=-\log(-\log\varepsilon^l_i),\, \varepsilon^l_i\sim \mathrm{Uniform}(0,1)$ , and a temperature  $\gamma>0$ , resulting in:

$$\boldsymbol{\beta}_{i}^{l}(\gamma) = \operatorname{softmax}_{i}\left(\frac{u_{i}^{l} + g_{i}^{l}}{\gamma}\right) = \frac{\exp\left(\left(u_{i}^{l} + g_{i}^{l}\right)/\gamma\right)}{\sum_{k=1}^{N} \exp\left(\left(u_{k}^{l} + g_{k}^{l}\right)/\gamma\right)}.$$
(5)

We combine these gates using a Straight-Through Estimator (STE) [17]. In the forward pass, we apply the deterministic

policy for stability:

$$m_i^l \text{-fwd} = \mathbb{I}[u_i^l \geq \tau] \cdot \mathsf{OneHot}\Big(i = \arg\max_k u_k^l\Big). \tag{6}$$

In the backward pass, we compute gradients as if the mask was the soft, differentiable approximation  $\tilde{m}_i^l = \alpha_i^l \beta_i^l(\gamma)$ .  $\gamma$  follows the same annealing schedule as  $\eta$  during training.

Inference-time Deterministic Policy. At inference, we apply the deterministic policy from the STE's forward pass. Each agent  $a_i$  applies the thresholding  $\tau$  on the meta utility map  $\mathbf{U}_i$  and exchanges the sparse meta utility map, on which the local scheduler applies the per-cell top-1 policy:

$$m_i^l = \mathbb{I}[u_i^l = \max_k u_k^l] \cdot \mathbb{I}[u_i^l \ge \tau]. \tag{7}$$

Let  $C_i^l$  be the cost (bytes) of sending  $\mathbf{f}_i^l$ , and  $\rho_i^l = u_i^l/C_i^l$  the utility—cost ratio. We sort all (i,l) with  $m_i^l = 1$  by  $\rho_i^l$  and admit the longest prefix whose cumulative cost  $\leq B$ .

**Proposition 1** (Consistency of differentiable and deterministic schedulers). For any (i,l) with  $u_i^l \neq \tau$  and with no injected noise at inference, we have

$$\lim_{\eta \to 0^+} \sigma\left(\frac{u_i^l - \tau}{\eta}\right) = \mathbb{I}[u_i^l > \tau],\tag{8}$$

$$\lim_{\gamma \to 0^+} \beta^l(\gamma) = \text{OneHot}\Big(i = \arg\max_k u_k^l\Big). \tag{9}$$

Therefore, we have

$$\lim_{\eta \to 0^+} \tilde{m}_i^l = \mathbb{I}[u_i^l = \max_k u_k^l] \cdot \mathbb{I}[u_i^l > \tau] = m_i^l. \tag{10}$$

Prop. (1) indicates that the train-time relaxed mask converges pointwise to the deterministic policy. Also, instead of a heuristic design, we show that this policy is provably optimal for the utility proxy in Eq. (4) and the knapsack problem under uniform costs.

**Theorem 1** (Singleton optimality). For each cell l, under the utility proxy in Eq. (4), any maximizer of  $U^l$  selects at most one agent:  $|\{i: m_i^l = 1\}| \le 1$ .

*Proof.* Order agents by  $u_1^l \geq u_2^l \geq \cdots$ . Selecting agent 1 yields  $U^l = u_1^l$ . Adding agent 2 changes utility by  $u_2^l - \min(u_1^l, u_2^l) = 0$ . Adding any  $k \geq 3$  to a set  $\mathcal S$  that already contains agent 1 and 2 yields marginal gain  $u_k^l - \sum_{j \in \mathcal S} \min(u_k^l, u_j^l) \leq u_k^l - \min(u_k^l, u_2^l) = 0$ .

Theorem (1) ensures that there is at most one agent with the highest utility to transmit per location cell, inherently eliminating cross-agent redundancy, as visualized in Fig. 3. This reduces the knapsack problem (C3) of selecting features across both agent and location dimensions to selecting the best set of location cells to transmit. Although the problem remains a knapsack problem, it becomes a uniform-cost

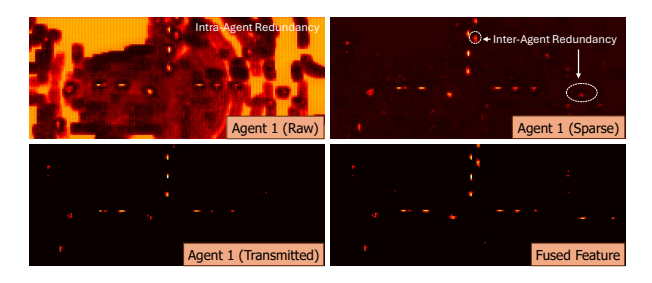


Figure 4. Visualization of feature map examples.

knapsack, since the number of channels is fixed per feature, resulting in the same transmission cost. It is known that the uniform-cost knapsack reduces to a cardinality-constrained selection, which can be optimally solved by taking the elements with the largest utilities [13], as shown in Theorem (2).

**Theorem 2** (Greedy optimality under equal costs). Suppose each feature (i,l) has the same nonzero cost  $C_i^l \equiv c > 0$ . Let the per-frame budget be B and define the integer capacity  $K \triangleq \lfloor B/c \rfloor$ . Then an optimal solution is obtained by selecting any K features with the largest utilities  $u_i^l$ .

*Proof.* By Theorem (1), each cell yields at most one admissible candidate; thus the global problem is

$$\max_{\mathcal{S} \subseteq \mathcal{C}} \sum_{(i,l) \in \mathcal{S}} u_i^l \quad \text{s.t.} \quad |\mathcal{S}| \le K, \tag{11}$$

where  $\mathcal C$  is the set of at-most-one-per-cell candidates and all costs equal c. This is a *cardinality-constrained* selection problem. Let  $\mathcal G$  be the greedy solution: the K items with the largest utilities. Assume for contradiction that  $\mathcal G$  is not optimal. Let  $\mathcal O$  be an optimal solution with  $|\mathcal O| \leq K$  and  $\sum_{o \in \mathcal O} u(o) > \sum_{g \in \mathcal G} u(g)$ . If  $|\mathcal O| < K$ , augment  $\mathcal O$  by adding the highest-utility items not in  $\mathcal O$  until its size reaches K; this cannot decrease its objective value because utilities are nonnegative, so w.l.o.g. take  $|\mathcal O| = K$ .

Order items in  $\mathcal{G}$  and  $\mathcal{O}$  so that  $u(g_1) \geq \cdots \geq u(g_K)$  and  $u(o_1) \geq \cdots \geq u(o_K)$ . Since  $\mathcal{G}$  contains the top-K utilities overall, we must have  $u(g_j) \geq u(o_j)$  for every  $j=1,\ldots,K$ . Summing over j yields  $\sum_{j=1}^K u(g_j) \geq \sum_{j=1}^K u(o_j)$ , contradicting  $\sum_{o \in \mathcal{O}} u(o) > \sum_{g \in \mathcal{G}} u(g)$ . Hence  $\mathcal{G}$  is optimal.

### 3.5. End-to-End Communication-Aware Training

We unify these components into an end-to-end trainable framework. The final loss combines the downstream task loss (*e.g.* focal, cross-entropy, etc.) with the semantic loss:

$$\mathcal{L}_{\text{JigsawComm}} = \mathcal{L}_{\text{task}} + \lambda \mathcal{L}_{\text{semantic}}, \tag{12}$$

where  $\lambda$  is a hyperparameter balancing the sparsity of the encoded feature and task accuracy. The  $\mathcal{L}_{task}$  gradient flows

through the differentiable scheduler (Sec. 3.4) to train the FUE head (Sec. 3.3), while  $\mathcal{L}_{\text{semantic}}$  shapes the encoder (Sec. 3.2). By learning the sparsity threshold  $\kappa$  and the utility threshold  $\tau$  jointly, JigsawComm learns to activate and transmit features only when they contribute to CP accuracy, maximizing the utility of every transmitted bit, as shown in Fig. 4.

### 4. Evaluation

### 4.1. Experimental Setup

**Dataset.** We evaluate JigsawComm on two CP datasets: (i) OPV2V [33], which is a large-scale benchmark collected across 70 diverse scenes from 8 towns in the digital twin simulator CARLA [4]. It includes 11,464 frames of LiDAR point cloud data from 2-5 agents and 232,913 annotated 3D bounding boxes. (ii) DAIR-V2X [34], which is the first large-scale real-world CP dataset for vehicle-infrastructure cooperation, consisted of 71,254 frames.

**Implementation Details.** We adopt PointPillars [15] as the LiDAR BEV backbone and a max-out module as the fusion backbone [3]. We train JIGSAWCOMM for up to 100 epochs using Adam ( $\beta_1=0.9,\beta_2=0.999$ ), with a base learning rate of 0.002. The Gumbel-Softmax temperatures  $\eta,\gamma$  are annealed from  $0.9 \rightarrow 0.1$ . We select  $\lambda=1000$  for OPV2V and  $\lambda=100$  for DAIR-V2X, through standard cross validation.

**Evaluation Metrics.** We evaluate 3D object detection performance using the mean Average Precision (mAP) at IoU thresholds of 0.5 and 0.7. Communication cost is measured by the Average Total Data Size (KB) transmitted per frame by all agents, under FP8. We also report Relative Communication Efficiency, defined as mAP@0.5/Total Size, normalized to our method (100%) for comparison. The required bandwidth is calculated as the total transmitted feature size multiplied by the frame rate (r=10 FPS).

**Baselines.** We follow the evaluation protocol that has become standard in communication-efficient CP [10, 19, 30, 39]: (i) a *no-fusion* single-vehicle detector, (ii) strong *full-transmission intermediate-fusion* methods that transmit dense BEV features, including F-Cooper [3], V2X-ViT [32], and AttFusion [33], and (iii) *communication-efficient CP* via Where2comm [9], which is the de facto canonical communication-efficient baseline adopted by recent works [10, 19, 30, 39]. Although some recent approaches [10, 19, 39] achieve comparable bandwidth requirements, they suffer from practical limitations in generalizability or computation latency, as discussed in Sec. 2.2.

### 4.2. Quantitative Results

**Main Results.** Table 2 presents our main results. On the OPV2V dataset, JIGSAWCOMM's accuracy matches or exceeds all baselines, including the top-performing full-transmission method, AttFusion. However, AttFusion achieves this by transmitting 22,792 KB per frame. JIGSAWCOMM achieves

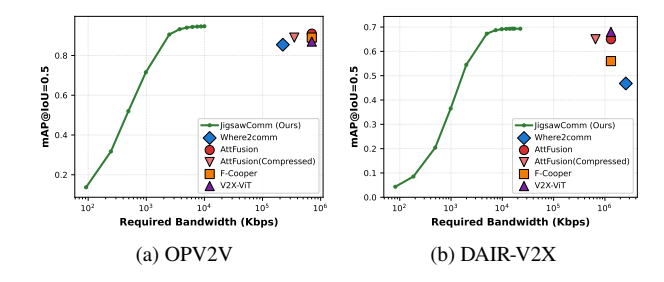


Figure 5. Tradeoff between accuracy and required bandwidth.

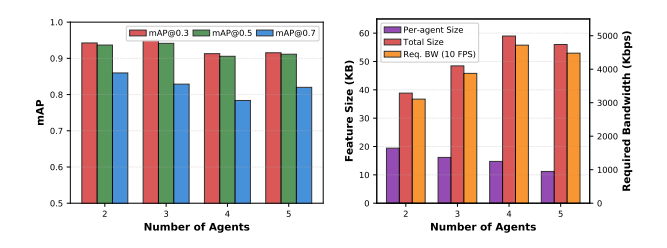


Figure 6. Accuracy, feature size, and required bandwidth grouped by agent counts on OPV2V. Instead of a linear increase in total feature size with more agents, JIGSAWCOMM induces an asymptotic  $\mathcal{O}(1)$  communication cost while achieving high accuracy.

this SOTA accuracy using only  $43.84~\mathrm{KB}$ , a  $520\times$  reduction. This highlights the severe inefficiency of baseline methods, which waste the majority of their bandwidth on non-essential or redundant data. On the real-world DAIR-V2X dataset, JIGSAWCOMM achieves the highest mAP@0.5, surpassing the best baseline, V2X-ViT, while using only 281.97 KB of data, a  $116\times$  reduction.

Accuracy-Bandwidth Tradeoff. Figure 5 visualizes JigsawComm's performance versus the required communication bandwidth (BW). The baselines are fixed points, representing inflexible, inefficient strategies. JigsawComm's curve is generated by varying the communication budget B. The accuracy of JigsawComm saturates quickly after  $BW \geq 1,000$  Kbps, making it a flexible, generalizable, and pragmatic solution for deployment under the limited bandwidth offered by V2X (e.g,  $\leq$ 20 Mbps) [6, 7].

Scalability with Number of Agents. JigsawComm achieves an asymptotic  $\mathcal{O}(1)$  communication cost, where the total bandwidth is bounded by the scene's information content in a single sparse feature, not the number of participating agents N. We validate this claim empirically in Fig. 6 using the OPV2V dataset, which includes 2 to 5 agents. JigsawComm's accuracy remains high as the number of agents varies. The total feature size grows slightly from  $\approx$ 40 KB at N=2 to  $\approx$ 58 KB at N=4, which is attributed to the fact that more agents increases collective scene coverage. Our FUE correctly identifies these non-redundant cells as having high utility and adds them to the 'jigsaw puzzle'.

Table 2. Main performance and communication efficiency comparison on the OPV2V and DAIR-V2X datasets. The relative communication efficiency is the normalized ratio between mAP@0.5 and average total data size. JIGSAWCOMM achieves SOTA performance while reducing communication volume by up to over  $500 \times$ . Note that, these results assume unlimited communication budget B.

Dataset	OPV2V					DAIR-V2X				
Model	mAP @0.5	mAP @0.7	Per-Agent Size (KB)	Total Data Size (KB)	Rel. Eff. (%)	mAP @0.5	mAP @0.7	Per-Agent Size (KB)	Total Data Size (KB)	Rel. Eff. (%)
No Fusion	0.68	0.60	-	-	- 1	0.50	0.44	-	-	_
F-Cooper	0.89	0.79	8,800.00	22,792.00	0.19	0.56	0.39	16,384.00	32,768.00	0.70
V2X-ViT	0.87	0.67	8,800.00	22,792.00	0.18	0.68	0.50	16,384.00	32,768.00	0.84
AttFusion(*)	0.91	0.82	8,800.00	22,792.00	0.19	0.65	0.51	16,384.00	32,768.00	0.81
(*) + Enc-Dec	0.89	0.81	4,400.00	11396.00	0.38	0.65	0.51	8,192.00	16,384.00	1.61
Where2comm	0.85	0.60	1,152.47	2,794.72	1.47	0.46	0.23	14,692.88	29,385.76	0.64
JigsawComm	0.92	0.82	17.46	43.84	100.00	0.69	0.52	148.96	281.97	100.00

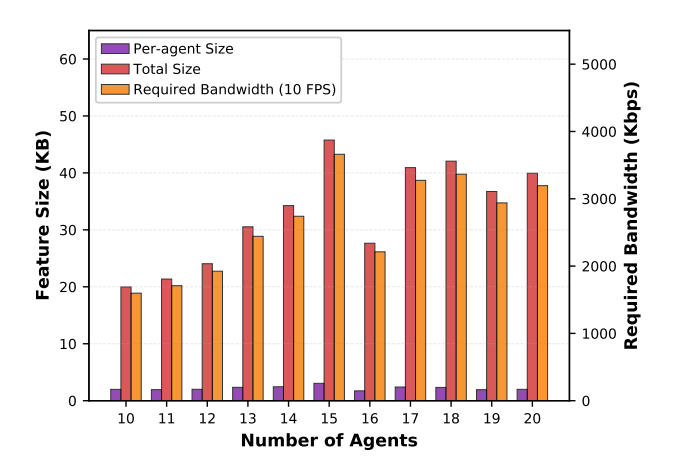


Figure 7. JIGSAWCOMM's total feature size and required bandwidth under 10 FPS on our custom dataset.

Since OPV2V is limited to 5 agents, we conduct further experiments on a custom-simulated dataset to analyze the asymptotic trend. We utilized the CARLA digital twin simulator [4] in conjunction with the OpenCDA framework [31] for coordinated multi-agent simulation and data recording. We set up the scene within CARLA's 'Town10HD' map with 10-20 CAVs following realistic traffic rules, at a large multi-lane intersection. The data was collected following the same format and conventions as the public OPV2V benchmark dataset, including sensor configurations, coordinate systems, and CAV parameters, to ensure compatibility with existing CP models and evaluation pipelines. Fig. 7 presents the result of JigsawComm on the custom dataset. We can observe that JigsawComm's total communication cost does not double when scaling from 10 to 20 agents. It saturates and remains relatively flat when the number of agents is greater than 15, empirically verifying the asymptotic  $\mathcal{O}(1)$  communication cost claim. As more agents join, the collective coverage saturates, the overlap becomes dominant, and the marginal contribution of each new agent becomes smaller.

Table 3. Ablation study of our core components.

Components		OPV	V2V	DAIR-V2X		
Semantic Loss	FUE & Sched.	mAP@0.5	Size (KB)	mAP@0.5	Size (KB)	
<b>√</b>	-	0.93	26,292.36	0.55	22,670.62	
-	✓	0.94	13,516.80	0.61	7,374.995	
$\checkmark$	$\checkmark$	0.92	43.84	0.69	279.97	

End-to-End Efficiency. Beyond theoretical bandwidth savings, we validate JigsawComm's end-to-end efficiency. The average end-to-end latency is  $45.82 \pm 26.96$  ms, which is well within the stringent 100 ms real-time budget for autonomous driving perception [16]. This total latency consists of  $28.27 \pm 23.88$  ms for computation on an RTX 4090 GPU and  $17.55 \pm 7.14$  ms for communication (assuming a 20 Mbps bandwidth constraint), including the total feature payload from all agents and the meta utility maps with a small total overhead of  $0.08 \pm 0.04$ KB.

#### 4.3. Ablation Study

Impact of Core Components. Table 3 ablates our two main contributions: the Semantic Loss  $\mathcal{L}_{\text{semantic}}$  and the FUE & Scheduling module. Removing the FUE & Scheduler still allows the encoder's  $\mathcal{L}_{\text{semantic}}$  to create sparse feature maps. However, the entire maps are transmitted, leading to redundancy and a large payload. Without  $\mathcal{L}_{\text{semantic}}$ , the FUE & Scheduler deal with dense and semantically-overloaded features, making it hard to select due to noisy utility estimates, still resulting in a large payload. Only with the presence of both components, the transmission size is greatly reduced while attaining high CP accuracy.

Effect of Redundancy. The system's transmission model is based on Theorem (1), demonstrating that selecting features from more than the Top-1 agent per cell is suboptimal. Fig. 8 validates this empirically. Comparing our Top-1 Agent policy to a Top-2 Agents policy, results show that Top-2 is worse at nearly every bandwidth point, indicating that transmitting redundant features wastes bandwidth and degrades percep-

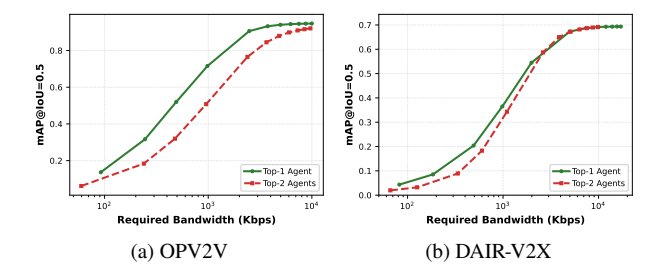


Figure 8. Ablation on number of agents sharing per cell. Including the agent with the second-highest utility does not improve the utility-bandwidth tradeoff, which corroborates Theorem (1).

tion accuracy. Although adding more data seems beneficial, this highlights a limitation in current fusion networks. Sec. 5 discusses this phenomenon and its implications further.

#### 5. Discussion

On the 'Cost' of Redundancy. A critical, counterintuitive finding from our evaluation is that transmitting from the Top-2 agents per cell yields worse performance than transmitting the Top-1 agent alone, as shown in Fig. 8. This 'more is worse' outcome stems from a fundamental limitation presented in current SOTA CP fusion algorithms, such as element-wise max-pooling or dot-product attention [3, 9, 33]. The fused feature is a weighted sum of the received features, with the informative activations in the fused feature upper-bounded by the maximum signal across the individual features. Therefore, unlike human vision, these methods struggle to synergetically fuse redundant information. If the second-best agent's feature is noisier or semantically different (e.g. conflicting channel activations), it can 'dilute' the clean, high-utility representation from the Top-1 agent. This finding corroborates the design philosophy of JigsawComm, which selects only the highest-quality, non-redundant data, resulting in smaller overhead and higher accuracy.

Why Not a Naive Communication Loss? A straightforward approach to reduce data size might be to add a simple communication loss directly on the transmission masks  $\{\mathbf{M}\}_{i=1}^N$ , penalizing the total number of transmitted bits. We found this approach to produce suboptimal performance in practice. Such a loss disregards the semantic importance and redundancy of the information transmitted, yet penalizes all communication. Our framework avoids this by training the FUE head to learn a task-aligned utility proxy, ensuring that selection decisions are driven by semantic-importance and redundancy.

Relation to Semantic Communications. JIGSAWCOMM is related to semantic/goal-oriented communications [1, 21, 27], since they share the high-level goal of task-oriented data compression. However, existing work in semantic communications targets different applications [27], considers only

single sensor perception [1, 21, 36], or neglects sensor correlations [25]. Applying semantic communications to CP involves unique challenges due to its collaborative and multisource input nature, where inter-agent redundancy prevails due to overlapping sensory data. Essentially, the CP problem studied in this paper can be reformulated as a joint, multisource, task-oriented data compression problem, which is difficult to solve without knowing a priori the exact interagent data correlation structure. JigsawComm solves this problem via a data-driven approach (with a small overhead of exchanging semantic feature utilities).

Meanwhile, the semantic regularization and redundancyeliminating transmission scheduling design of JigsawComm can be viewed as a way of implementing the information bottleneck (IB) principle, where unnecessary information is minimized while task-relevant information is maximized, which is essential to achieve goal-oriented communications [21, 27]. Interestingly, the same IB principle has also been shown to be effective in reducing generalization errors in deep learning models [12]. Here, our end-to-end trained JIGSAWCOMM learns to keep only semantically-relevant information from its sparse encoder and selects non-redundant and high-utility features for transmission, which effectively controls the IB of the CP pipeline. Therefore, in addition to the drastic reduction in required bandwidth for real-time communication, JigsawComm also achieves matching or improved perceptual quality compared to full-feature baselines. **Practical Implementation.** Our framework is designed for practical V2X implementation by leveraging its dualchannel architecture [6, 7]. The meta utility maps, though scaling linearly with agent count, can be transmitted over the control channel, incurring negligible overhead (<0.03 KB per agent under 4-bit quantization). The final, sparse BEV features are then sent efficiently over the data channel, such as via the Collective Perception Message (CPM) defined by ITS [5]. Note that, our scheduler outputs the transmission priorities of all agents' selected features as a byproduct (ordered by the corresponding feature utility values), which

### 6. Conclusion and Future Work

agent in a distributed manner.

We present JigsawComm, a novel joint semantic feature encoding and transmission framework for CP that maximizes every transmitted bit's contribution to the final task accuracy. By jointly training a semantic sparse encoder and a lightweight Feature Utility Estimator via a differentiable

can be easily integrated into the low-layer V2X protocols for

both scheduling-based (e.g. C-V2X, 5G NR-V2X [6, 8]) and

random-access V2X protocols (e.g. DSRC [7]). Our scheme

is compatible with both centralized (V2I) and decentralized

(V2V) operating modes. For V2I, an edge server co-located

with the RSU can perform scheduling, fusion, and inference.

For V2V, the same set of computations is performed by each

scheduler, JigsawComm learns to extract and select only essential, non-redundant data. This enables a provably optimal top-1 policy at inference that eliminates cross-agent redundancy and achieves a scalable  $\mathcal{O}(1)$  communication cost. Our experiments on OPV2V and DAIR-V2X demonstrate SOTA accuracy with up to over  $500\times$  bandwidth reduction.

There are several promising directions for future work. First, as JigsawComm adopts the index-based encoding to convert sparsely encoded features to bits, we will further push the limit of JigsawComm's bandwidth efficiency by integrating traditional lossless source coding methods such as entropy coding [26]. Second, we will also extend JigsawComm with joint semantic source and channel coding to deal with unreliable channel conditions. Third, we will study the impact of different sensor modalities and feature cell granularities on the accuracy-bandwidth tradeoff, and explore novel fusion networks that can leverage, rather than suffer from, redundancy. Finally, we will study practical V2X-based CP system design, robustness to communication failures or packet losses, and end-to-end goal-oriented CP systems for autonomous driving.

### References

- [1] Francesco Binucci, Paolo Banelli, Paolo Di Lorenzo, and Sergio Barbarossa. Adaptive resource optimization for edge inference with goal-oriented communications. *EURASIP Journal on Advances in Signal Processing*, 2022(1), 2022. 9
- [2] Ioannis Chatziioannou, Stefanos Tsigdinos, Panagiotis G. Tzouras, Alexandros Nikitas, and Efthimios Bakogiannis. Connected and autonomous vehicles and infrastructure needs: Exploring road network changes and policy interventions. In *Deception in Autonomous Transport Systems:* Threats, Impacts and Mitigation Policies. Springer, 2024. 1
- [3] Qi Chen, Xu Ma, Sihai Tang, Jingda Guo, Qing Yang, and Song Fu. F-cooper: feature based cooperative perception for autonomous vehicle edge computing system using 3D point clouds. In *Proc. of the ACM/IEEE Symposium on Edge Computing (SEC)*, 2019. 1, 2, 3, 7, 9
- [4] Alexey Dosovitskiy, German Ros, Felipe Codevilla, Antonio Lopez, and Vladlen Koltun. CARLA: An open urban driving simulator. In *Proc. of the Conference on Robot Learning* (*CoRL*), 2017. 7, 8
- [5] European Telecommunications Standards Institute (ETSI). Intelligent transport system (its); vehicular communications; basic set of applications; collective perception service; release 2, 2023. Release 2. 1, 9
- [6] European Telecommunications Standards Institute (ETSI). ETSI EN 303 613 V1.1.1: Intelligent Transport Systems (ITS); Congestion Control Mechanisms for C-V2X PC5 Interface; Access Layer Part, 2019. [Online]. 1, 3, 7, 9
- [7] Federal Communications Commission (FCC). Dedicated Short Range Communications (DSRC) Service, 2025. [Online]. 1, 3, 7, 9
- [8] Mario H Castañeda Garcia, Alejandro Molina-Galan, Mate Boban, Javier Gozalvez, Baldomero Coll-Perales, Taylan

- Şahin, and Apostolos Kousaridas. A tutorial on 5G NR V2X communications. *IEEE Communications Surveys & Tutorials*, 2021. 9
- [9] Yue Hu, Shaoheng Fang, Zixing Lei, Yiqi Zhong, and Siheng Chen. Where2comm: Communication-efficient collaborative perception via spatial confidence maps. Advances in Neural Information Processing Systems (NeurIPS), 2022. 1, 2, 3, 4, 7, 9
- [10] Yue Hu, Juntong Peng, Sifei Liu, Junhao Ge, Si Liu, and Siheng Chen. Communication-efficient collaborative perception via information filling with codebook. In *Proc. of* the IEEE/CVF Conference on Computer Vision and Pattern Recognition (CVPR), 2024. 1, 3, 7
- [11] Eric Jang, Shixiang Gu, and Ben Poole. Categorical reparameterization with gumbel-softmax. *arXiv preprint* arXiv:1611.01144, 2016. 5
- [12] Kenji Kawaguchi, Zhun Deng, Xu Ji, and Jiaoyang Huang. How does information bottleneck help deep learning? In Proc. of the International Conference on Machine Learning (ICML), 2023.
- [13] Hans Kellerer, Ulrich Pferschy, and David Pisinger. Multidimensional knapsack problems. In *Knapsack problems*, pages 235–283. Springer, 2004. 4, 6
- [14] Seong-Woo Kim, Wei Liu, Marcelo H. Ang, Emilio Frazzoli, and Daniela Rus. The impact of cooperative perception on decision making and planning of autonomous vehicles. *IEEE Intelligent Transportation Systems Magazine*, 7(3):39– 50, 2015. 1
- [15] Alex H Lang, Sourabh Vora, Holger Caesar, Lubing Zhou, Jiong Yang, and Oscar Beijbom. Pointpillars: Fast encoders for object detection from point clouds. In Proc. of the IEEE/CVF Conference on Computer Vision and Pattern Recognition (CVPR), 2019. 7
- [16] Shih-Chieh Lin, Yunqi Zhang, Chang-Hong Hsu, Matt Skach, Md E. Haque, Lingjia Tang, and Jason Mars. The architectural implications of autonomous driving: Constraints and acceleration. In Proc. of the International Conference on Architectural Support for Programming Languages and Operating Systems (ASPLOS). ACM, 2018. 1, 3, 8
- [17] Mingju Liu, Yingjie Li, Jiaqi Yin, Zhiru Zhang, and Cunxi Yu. Differentiable combinatorial scheduling at scale. In Proc. of the International Conference on Machine Learning (ICML), 2024. 5
- [18] Yen-Cheng Liu, Junjiao Tian, Nathaniel Glaser, and Zsolt Kira. When2com: Multi-agent perception via communication graph grouping. In Proc. of the IEEE/CVF Conference on Computer Vision and Pattern Recognition (CVPR), 2020. 1, 3, 4
- [19] Ruiqing Mao, Haotian Wu, Yukuan Jia, Zhaojun Nan, Yuxuan Sun, Sheng Zhou, Deniz Gündüz, and Zhisheng Niu. Diffcp: Ultra-low bit collaborative perception via diffusion model. In *Proc. of the International Conference on Robotics and Automation (ICRA)*. IEEE, 2025. 3, 7
- [20] Andrew Y Ng. Feature selection, 11 vs. 12 regularization, and rotational invariance. In *Proc. of the International Conference* on Machine Learning (ICML), 2004. 5
- [21] Francesco Pezone, Sergio Barbarossa, and Paolo Di Lorenzo. Goal-oriented communication for edge learning based on the

- information bottleneck. In *Proc. of the International Conference on Acoustics, Speech and Signal Processing (ICASSP)*. IEEE, 2022. 9
- [22] Zhijin Qin, Xiaoming Tao, Jianhua Lu, Wen Tong, and Geoffrey Ye Li. Semantic communications: Principles and challenges. arXiv preprint arXiv:2201.01389, 2021. 5
- [23] Hang Qiu, Pohan Huang, Namo Asavisanu, Xiaochen Liu, Konstantinos Psounis, and Ramesh Govindan. AutoCast: Scalable infrastructure-less cooperative perception for distributed collaborative driving. In Proc. of the International Conference on Mobile Systems, Applications, and Services (MobiSys), 2022. 3
- [24] Andreas Rauch, Felix Klanner, Ralph Rasshofer, and Klaus Dietmayer. Car2x-based perception in a high-level fusion architecture for cooperative perception systems. In *Proc. of the IEEE Intelligent Vehicles Symposium*, 2012. 3
- [25] Yucheng Sheng, Hao Ye, Le Liang, Shi Jin, and Geoffrey Ye Li. Semantic communication for cooperative perception based on importance map. *Journal of the Franklin Institute*, 361(6), 2024. 4, 9
- [26] James A Storer. Data compression: methods and theory. Computer Science Press, Inc., 1988. 10
- [27] Emilio Calvanese Strinati and Sergio Barbarossa. 6G networks: Beyond Shannon towards semantic and goal-oriented communications. *Computer Networks*, 2021. 5, 9
- [28] Wanfang Su, Lixing Chen, Yang Bai, Xi Lin, Gaolei Li, Zhe Qu, and Pan Zhou. What makes good collaborative views? contrastive mutual information maximization for multi-agent perception. In *Proc. of the AAAI Conference on Artificial Intelligence (AAAI)*, 2024. 3
- [29] Ruiqi Wang and Guohong Cao. Edge-assisted camera selection in vehicular networks. In *Proc. of the IEEE Conference on Computer Communications (INFOCOM)*, 2024. 3
- [30] Junhao Xu, Yanan Zhang, Zhi Cai, and Di Huang. CoSDH: Communication-efficient collaborative perception via supply-demand awareness and intermediate-late hybridization. In Proc. of the IEEE/CVF Conference on Computer Vision and Pattern Recognition (CVPR), 2025. 1, 3, 4, 7
- [31] Runsheng Xu, Yi Guo, Xu Han, Xin Xia, Hao Xiang, and Jiaqi Ma. Opencda: An open cooperative driving automation framework integrated with co-simulation. In *Proc. of the IEEE International Intelligent Transportation Systems Conference (ITSC)*, 2021. 8
- [32] Runsheng Xu, Hao Xiang, Zhengzhong Tu, Xin Xia, Ming-Hsuan Yang, and Jiaqi Ma. V2X-ViT: Vehicle-to-everything cooperative perception with vision transformer. In *Proc. of the European Conference on Computer Vision (ECCV)*, 2022. 2, 3, 7
- [33] Runsheng Xu, Hao Xiang, Xin Xia, Xu Han, Jinlong Li, and Jiaqi Ma. OPV2V: An open benchmark dataset and fusion pipeline for perception with vehicle-to-vehicle communication. In *Proc. of the International Conference on Robotics and Automation (ICRA)*, 2022. 1, 2, 3, 7, 9
- [34] Haibao Yu, Yizhen Luo, Mao Shu, Yiyi Huo, Zebang Yang, Yifeng Shi, Zhenglong Guo, Hanyu Li, Xing Hu, Jirui Yuan, et al. Dair-v2x: A large-scale dataset for vehicle-infrastructure cooperative 3d object detection. In *Proc. of*

- the IEEE/CVF Conference on Computer Vision and Pattern Recognition (CVPR), 2022. 7
- [35] Haibao Yu, Yingjuan Tang, Enze Xie, Jilei Mao, Ping Luo, and Zaiqing Nie. Flow-based feature fusion for vehicleinfrastructure cooperative 3d object detection. Advances in Neural Information Processing Systems (NeurIPS), 2023. 3
- [36] Zhongzheng Yuan, Siddharth Garg, Elza Erkip, and Yao Wang. Scalable feature compression for edge-assisted object detection over time-varying networks. In *In MLSys Workshop on Resource-Constrained Learning in Wireless Networks*, 2023. 9
- [37] Qingzhao Zhang, Xumiao Zhang, Ruiyang Zhu, Fan Bai, Mohammad Naserian, and Z Morley Mao. Robust realtime multi-vehicle collaboration on asynchronous sensors. In Proc. of the Annual International Conference on Mobile Computing and Networking (MobiCom), 2023. 2
- [38] Xumiao Zhang, Anlan Zhang, Jiachen Sun, Xiao Zhu, Y Ethan Guo, Feng Qian, and Z Morley Mao. Emp: Edgeassisted multi-vehicle perception. In Proc. of the Annual International Conference on Mobile Computing and Networking (MobiCom), 2021. 2, 3
- [39] Seth Z Zhao, Huizhi Zhang, Zhaowei Li, Juntong Peng, Anthony Chui, Zewei Zhou, Zonglin Meng, Hao Xiang, Zhiyu Huang, Fujia Wang, et al. QuantV2X: A fully quantized multi-agent system for cooperative perception. arXiv preprint arXiv:2509.03704, 2025. 1, 3, 7